



OPEN SNHG6 facilitates the epithelial-mesenchymal transition and metastatic potential of esophageal squamous carcinoma through miR-26b-5p/ ITGB1 axis

Jiali Wang¹, Jiaxin Si¹, Ziyuan Zhao¹, Changlin Gao¹, Tianxu Liu¹, Yunlong Jia¹ & Lihua Liu^{1,2}✉

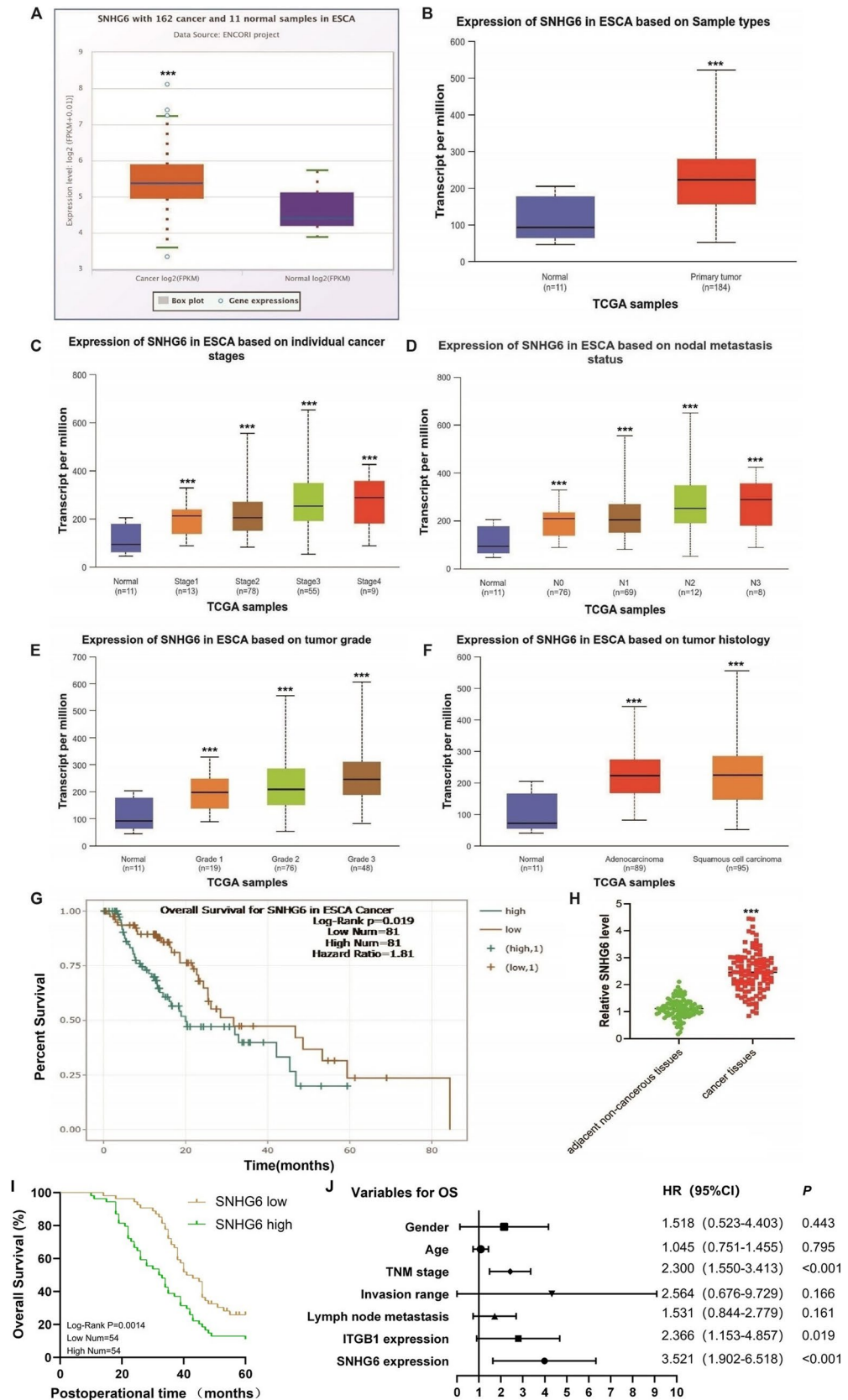
Long non-coding RNAs (lncRNAs), such as SNHG6, have been identified as crucial regulators in the progression of various cancers, including esophageal squamous cell carcinoma (ESCC). Although the role of SNHG6 in ESCC is not completely understood, our findings demonstrated that SNHG6 expression is upregulated in ESCC tissues compared to adjacent normal tissues. Furthermore, elevated levels of SNHG6 are significantly correlated with higher TNM stage and poorer clinical prognosis in ESCC patients. Functionally, both *in vivo* and *in vitro* experiments have shown that knocking down SNHG6 inhibits proliferation, invasion, and metastasis. Luciferase reporter assays and Ago2-RIP assay confirm that SNHG6 functions as a competing endogenous RNA (ceRNA) by sponging miR-26b-5p to modulate ITGB1 expression in ESCC. Given that ITGB1 is instrumental in EMT and metastasis, we assessed the expression of EMT-related proteins. The findings suggest that miR-26b-5p and reduced ITGB1 expression can reverse the EMT induced by lncRNA SHNG6, as demonstrated through rescue analysis. Overall, this study aims to elucidate the molecular mechanisms through which SNHG6 promotes EMT and metastasis in ESCC, providing a novel theoretical foundation for understanding ESCC progression and identifying new targets for improving outcomes in metastatic ESCC.

Keywords Esophageal squamous carcinoma, SNHG6, MiR-26b-5p/ITGB1, EMT

Esophageal squamous carcinoma (ESCC) is a malignancy with an increasingly high prevalence and is a leading cause of cancer-related deaths worldwide¹. Despite significant advances in oncological treatments, including combined multi-disciplinary management, the prognosis for ESCC remains poor with a 5-year overall survival rate of about 15%². Distant metastasis constitutes the primary obstacle to improving therapeutic outcomes. Therefore, developing more effective strategies through a better understanding of the molecular mechanisms underlying metastasis is crucial.

Long non-coding RNAs (lncRNAs) are identified as a class of RNA molecules exceeding 200 nucleotides in length with limited protein-coding capacity³. Numerous studies have demonstrated that lncRNAs are involved in wide array of biological functions, including cell migration, cellular phenotypic transformation, drug resistance, and disease pathogenesis⁴⁻⁶. Recent research has identified many lncRNAs acting as oncogenes or tumor suppressor genes in ESCC. For instance, lncRNA-DGCR5 acts as a potential oncogene in ESCC, significantly enhancing ESCC cell progression by inhibits TTP's anti-inflammatory activity⁷. Additionally, Cui Y. et al. showed that m6A-mediated epigenetic modification of lncRNA contributes to the tumorigenesis in ESCC and LINC00022, specific target of m6A, serves as a potential biomarker for this malignancy⁸. lncRNAs participate in nearly every regulatory step of gene expression, including chromatin remodeling, transcriptional control, splicing regulation, mRNA stability, mRNA translation, microRNA processing, DNA damage, and drug resistance⁹⁻¹⁴. Recently, lncRNAs have been recognized for their role in miRNA binding site sponging, leading to the concept of competing endogenous RNA (ceRNA)¹⁵. Specifically, many lncRNAs have been shown to indirectly regulate gene expression by functioning as ceRNA in the progression of ESCC.

¹Department of Tumor Immunotherapy, Hebei Medical University Fourth Affiliated Hospital, Hebei Provincial Tumor Hospital, Shijiazhuang 050035, China. ²China International Cooperation Laboratory of Stem Cell Research, Hebei Medical University, Shijiazhuang 050011, China. ✉email: cdlihua@hebmu.edu.cn



SnRNA host gene 6 (SHNG6), a recently identified lncRNA, acts as a contributor in various cancers and as a tumorigenic oncogene in ESCC¹⁶. Notably, the role of SNHG6 in the progression of colorectal cancer (CRC) has been confirmed by recent studies. SNHG6 exhibits oncogenic effects by acting as a ceRNA to sequester various miRNAs. For example, SNHG6 enhances proliferation, invasion and migration in breast cancer cells by modulating miR-543-3p/LAMC1 axis¹⁷. However, the molecular mechanisms by which SNHG6 contributes to

◀ **Figure 1.** SNHG6 is upregulated in esophageal squamous carcinoma tissues and is associated with poor prognosis. **A** The starBase database result showed that SNHG6 expression was significantly upregulated in ESCA tissues compared with normal tissues. **B-F** The UALCAN database results showed that SNHG6 expression was significantly upregulated in different ESCA clinical stages, lymph node metastasis status, tumor grades, and molecular subtypes. **G** The OS curves of ESCC patients were generated by Kaplan-Meier analysis from TCGA database. Elevated SNHG6 expression was correlated to a poor prognosis in patients. **H** SNHG6 expression validated by qRT-PCR in an independent cohort of 108 pairs of esophageal squamous carcinoma tissues and matched adjacent normal tissues. **I** The OS curves of ESCC patients were generated by Kaplan-Meier analysis. **J** Cox proportional hazards analysis to explore the factors influencing prognosis in patients with ESCC. * $P < 0.05$.

metastasis, particularly EMT, warrant further exploration. In this study, we elucidate the biological function and molecular mechanism of SNHG6 in ESCC. SNHG6 is significantly upregulated in ESCC tissues and is associated with poor prognosis. Functional assays demonstrate EMT and the progression of ESCC cells both *in vitro* and *in vivo*. Furthermore, mechanistic studies reveal that SNHG6 acts as a ceRNA to modulate the expression and activity of ITGB1 by competitively binding with miR-26b-5p. In conclusion, SNHG6 is an oncogenic regulator of ESCC EMT and progression, representing a potential biomarker and therapeutic target.

Results

Upregulation of SNHG6 is related to poor prognosis in ESCC To explore the potential role of SNHG6 in ESCC, we initially examined its expression status in ESCA tissues using the TCGA and starBase databases, revealing a marked elevation in SNHG6 levels in ESCA tissues (Fig. 1A). Further analysis utilizing the UALCAN database demonstrated that SNHG6 expression was significantly higher in patients with advanced clinical stages, lymph node metastasis, and poorer tumor grades (Fig. 1B-E). Meanwhile, it was discovered that SNHG6 was aberrantly highly expressed in ESCC tissues (Fig. 1F). Kaplan-Meier analysis indicated that high SNHG6 expression levels were associated with lower survival rates in ESCC patients (Fig. 1G).

To corroborate these findings, RT-qPCR was conducted on 108 pairs of ESCC tissues and adjacent non-cancerous tissues, confirming significantly elevated SNHG6 expression in the ESCC samples (Fig. 1H). The 108 human ESCC samples were subsequently categorized into two groups based on the median relative SNHG6 expression ratio: a high SNHG6 group ($n = 54$) and a low SNHG6 group ($n = 54$). SNHG6 expression was significantly correlated with TNM stage, lymph node metastasis, and tumor differentiation (Table 1). Additionally, we confirmed that higher SNHG6 expression levels were associated with worse outcomes (Fig. 1I). Subsequently, we conducted a Cox proportional hazards analysis and identified that both SNHG6 expression and TNM stage serve as independent prognostic factors for overall survival in patients with ESCC (Fig. 1J). Collectively, these results suggest that SNHG6 is aberrantly upregulated in ESCC and correlates with advanced TNM stage and poor prognosis, supporting an oncogenic role for SNHG6 in ESCC.

Knockdown SNHG6 inhibited ESCC cells proliferation, migration and invasion To elucidate the biological function of SNHG6 in ESCC cells, we measured its expression level across various ESCC cell lines (TE1, YES-2, Eca9706 and KYSE150) using qRT-PCR. SNHG6 was consistently expressed in these cell lines compared to the normal esophageal epithelial cell line HEEC (Fig. 2A). Notably, TE1 and Eca9706 exhibited the highest SNHG6 expression levels, prompting us to conduct RNAi experiments in these two cell lines. We initially transfected si-SNHG6 into the ESCC cells to assess its biological roles. Relative to the negative control siRNA group, si-SN-

	Total (n)	High expression of SNHG6 (n/%)	Low expression of SHNG6 (n/%)	P
Gender				0.441
Male	52	28 (53.85)	24 (46.15)	
Female	56	26 (46.43)	30 (53.57)	
Age				0.673
≤60	76	39 (51.32)	37 (48.68)	
>60	32	15 (46.88)	17 (53.12)	
TNM stage				0.038
I+II	74	32 (43.24)	42 (56.76)	
III	34	22 (64.71)	12 (35.29)	
Invasion range				0.014
T1+T2	72	30 (41.67)	42 (58.33)	
T3+T4	36	24 (66.67)	12 (33.33)	
Lymph node metastasis				0.003
Negative	45	15 (33.33)	30 (66.67)	
Positive	63	39 (61.90)	24 (38.10)	

Table 1. Association of SNHG6 expression with clinical parameters of ESCC patients. Note: * $P < 0.05$.

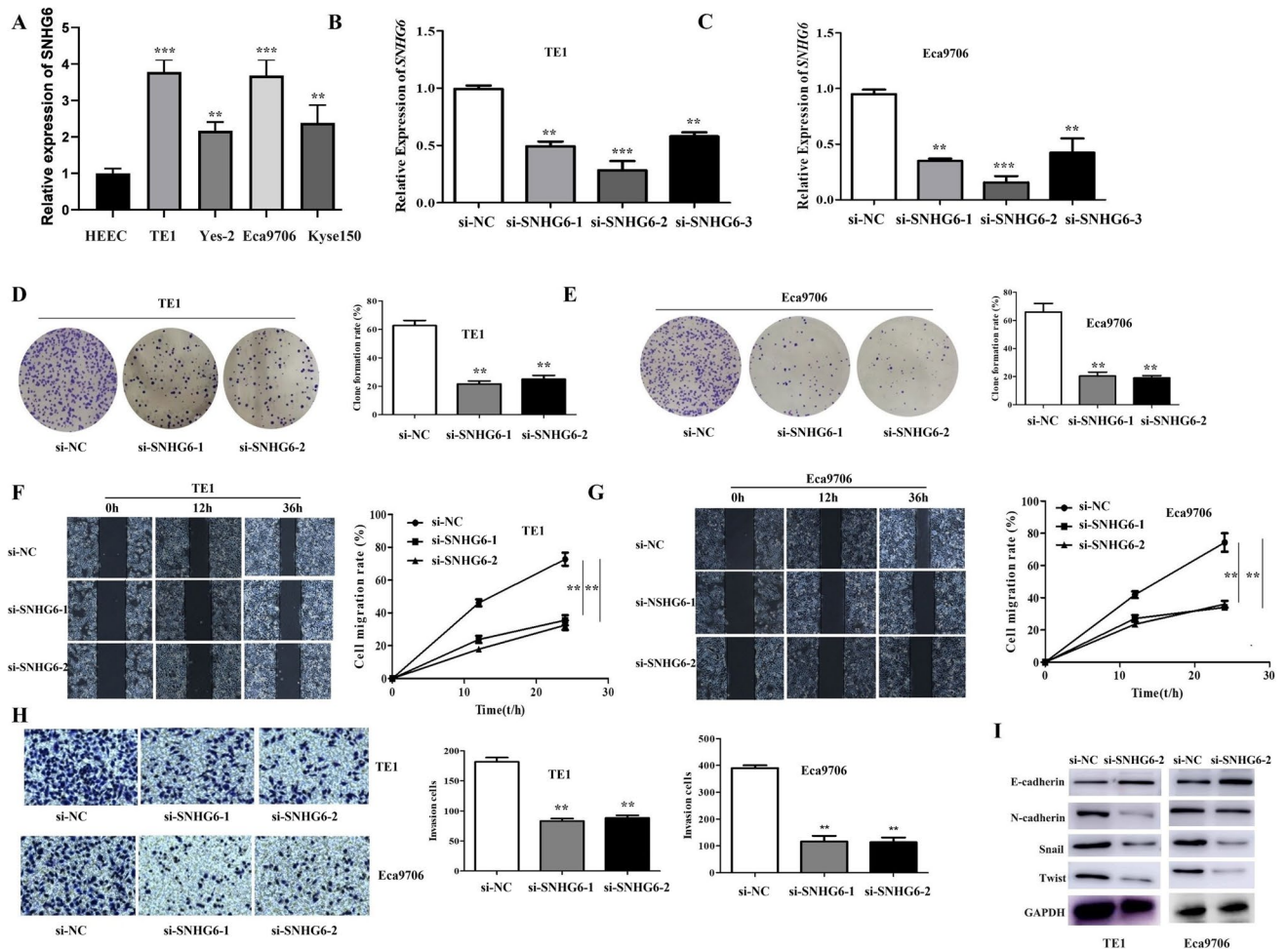


Figure 2. SNHG6 promotes ESCC cell proliferation and metastasis in vitro. **A** qRT-PCR analysis of SNHG6 expression in ESCC cells. **B–C** Relative expression of SNHG6 in ESCC cells transfected with SNHG6 siRNA (si-SNHG6-1, si-SNHG6-2 or si-SNHG6-3) and scrambled siRNA. **D–E** Proliferation of ESCC cells transfected with SNHG6 siRNA or scrambled siRNA as determined by colony formation assay. **F–H** Migration and invasion ability of TE1 and Eca9706 cells transfected with SNHG6 siRNA and scrambled siRNA as determined by wound healing and Transwell assays. **I** Expression of E-cadherin, N-cadherin, Snail and Twist in ESCC cells transfected with SNHG6 siRNA and scrambled siRNA. * $P < 0.05$.

HG6-1 and si-SNHG6-2 significantly reduced SNHG6 expression, while si-SNHG6-3 achieved a moderate reduction (Fig. 2B and C). Consequently, si-SNHG6-1 and si-SNHG6-2 were selected for subsequent experiments.

Intriguingly, knockdown of SNHG6 significantly suppresses cell proliferation in both TE1 and Eca9706 cells, as demonstrated by colony formation assays (Fig. 2D–E). To assess the impact of SNHG6 on the migration and invasive capabilities of ESCC cells, wound healing and Transwell assays were conducted using Eca9706 and TE1 cells lines. In TE1 cells, the migration index was significantly reduced by si-SNHG6-1 and si-SNHG6-2 compared to the si-NC group (Fig. 2F). Similarly, in Eca9706 cells, these variants also substantially decreased the migration index relative to the si-NC group (Fig. 2G). Concurrently, si-SNHG6-1 and si-SNHG6-2 markedly reduced the invasion cell count in TE1 cells compared to the si-NC group (Fig. 2H). For Eca9706 cells, these variants also significantly decreased the migration index compared to the si-NC group (Fig. 2H). Overall, the data indicate that SNHG6 knockdown effectively inhibits both migration and invasion of ESCC cells in vitro.

Knockdown SNHG6 suppressed EMT of ESCC cells Furthermore, the expression levels of EMT-related proteins (E-cadherin, N-cadherin, Snail, and Twist) were assessed using a western blotting assay. The results indicated that SNHG6 knockdown reduced the expression of N-cadherin, Snail, and Twist, while it increased the expression of E-cadherin expression in TE1 and Eca9706 cells at the protein level (Fig. 2I). These findings suggest that SNHG6 knockdown impedes the EMT process.

Knockdown SNHG6 inhibited the progression of ESCC cells via regulating miR-26b-5p Mounting research suggests that lncRNAs can functions by interacting with RNA-binding proteins or acting as a ceRNA for microRNAs (miRNAs). To elucidate the specific molecular mechanisms through which SNHG6 enhances ESCC

cell metastasis and progression, we initially investigated its localization in ESCC cells using fluorescence in situ hybridization (FISH) assay. The result revealed that SNHG6 predominantly localizes to the cytoplasm in TE1 cells (Fig. 3A), indicating that SNHG6 might regulate target protein expression at the posttranscriptional level.

Together, these findings suggest that SNHG6 may act as a ceRNA for miRNAs. Therefore, we utilized the bioinformatics databases webserver starBase (<https://starbase.sysu.edu.cn/>) to predict potential interactions between miRNAs and SNHG6. The data indicated that SNHG6 contains numerous miRNA binding sites. Subsequently, we analyzed the enrichment pathways of the ceRNA regulatory network of SNHG6 through starBase and found that the SNHG6-ceRNA regulatory network was mainly enriched in Focal adhesion, ECM-receptor interaction, and cell adhesion molecules. We identified miR-26b-5p, which is closely related to the above pathways, for further study (Fig. 3B-C). Then, we detected the subcellular location of miR-26b-5p in TE1 cells by performing FISH assay. The results showed that miR-26b-5p and SNHG6 were co-localized in the cytoplasm in TE1 cells (Fig. 3A). Then, we conducted Ago2-RIP and qRT-PCR assays to validate whether SNHG6 and miR-26b-5p occupied the same RNA-induced silencing complex (RISC). The outcomes revealed that the expressions of SNHG6 and miR-26b-5p were significantly elevated in Ago2 pellets compared with those in IgG pellets (Fig. 3D), suggesting that SNHG6 might function as a ceRNA to sponge miR-26b-5p and form a RISC in ESCC cells. Furthermore, the results of the luciferase reporter assay demonstrated that the miR-26b-5p mimics decreased the luciferase activity of SNHG6 in TE1 and Eca9706 cells transfected with SNHG6-WT or SNHG6-Mut (Fig. 3E).

Furthermore, we examined the expression status of miR-26b-5p in ESCC tissues and observed attenuation in its expression (Fig. 3F). To further substantiate the relationship between miR-26b-5p and SNHG6, we assessed their expression in ESCC cells. The results indicated a relative attenuation of miR-26b-5p across all ESCC cells compared to HEEC cells (Fig. 3G). Subsequently, we evaluated miR-26b-5p expression in ESCC cell lines following SNHG6 silencing, revealing a marked increase in miR-26b-5p expression (Fig. 3H). Collectively, these findings suggest that SNHG6 may act as a ceRNA to regulate miR-26b-5p, potentially influencing the expression of its target mRNA.

ITGB1 is a target gene of miR-26b-5p To investigate the role of miR-26b-5p in ESCC cells, we transfected miR-26b-5p mimic into ESCC cells and conducted colony formation assay. The findings demonstrated that expression of miR-26b-5p significantly inhibited cell proliferation and colony formation in these cells (Fig. 4A-C). Moreover, migration and invasion were also reduced in ESCC cells with high expression of miR-26b-5p (Fig. 4C-D).

To evaluate the ceRNA network involving SNHG6, miR-26b-5p, and their targets in ESCC, starBase (<https://starbase.sysu.edu.cn/>) was utilized to predict potential miR-26b-5p target genes using default settings. The prediction suggested ITGB1 as a target of miR-26b-5p in ESCC, revealing one hypothetical miR-26b-5p binding site within the ITGB1 3'-untranslated region (UTR) (Fig. 4E). To confirm our target, we conducted a luciferase reporter assay using the wild-type 3'-UTR sequence of ITGB1, incorporating the predicted miR-26b-5p binding sites (ITGB1-Wt), and mutant constructs with alterations in these sites (Mut). These plasmids were co-transfected into TE1 cells with either miR-26b-5p mimic or a negative control. The results indicated that the miR-26b-5p mimic specifically reduced luciferase activity driven by ITGB1-Wt, with no effect observed for the negative control mimic or ITGB1-Mut (Fig. 4F). Further analysis to determine if ITGB1 is regulated by miR-26b-5p in ESCC cells involved measuring ITGB1 mRNA and protein levels following miR-26b-5p knockdown or overexpression. Notably, ITGB1 mRNA levels were significantly reduced in TE1 and Eca9706 cells overexpressing miR-26b-5p (Fig. 4G).

Furthermore, to confirm the clinical significance of ITGB1 in ESCC, our study detected the expression level of ITGB1 in ESCC tissues and found that the expression level of ITGB1 was significantly higher in ESCC tissues than in adjacent tissues (Fig. 4H). Furthermore, we performed a Cox proportional hazards analysis and identified that ITGB1 serves as an independent prognostic factor for overall survival in patients with ESCC (Fig. 1J). Next, to clarify the relationship between the expression levels of SNHG6, miR-26b-5p, and ITGB1 in ESCC tissues, we conducted a correlation analysis. The results showed that ITGB1 was positively correlated with SNHG6, while negatively correlated with miR-26b-5p (Supplemental Fig. 1A-B). In conclusion, these findings demonstrate that miR-26b-5p directly targets the 3' UTR of ITGB1 mRNA, regulating ITGB1 expression in ESCC cells.

SNHG6 facilitates ESCC cell EMT, metastasis and progression by sponging miR-26b-5p to regulate ITGB1 functions To determine whether miR-26b-5p/ITGB1 is involved in the function of SNHG6 in ESCC cells, we co-transfected sh-SNHG6 (Supplemental Fig. 1C) with a miR-26b-5p inhibitor into Eca9706 cells. As depicted in Fig. 5A and B, the sh-SNHG6-mediated suppression of proliferation and metastasis was partially reversed by co-transfection with the miR-26b-5p inhibitor. Concurrently, the expression levels of EMT-related proteins (N-cadherin, Snail, Twist and E-cadherin) were partially restored upon co-transfection with the miR-26b-5p inhibitor, as shown in Fig. 5C. This suggests that SNHG6 promotes cell EMT and metastasis, at least partly, by inhibiting miR-26b-5p function.

ITGB1 is targeted by miR-26b-5p, prompting us to explore whether SNHG6 could regulate the ITGB1 expression by competitively binding miR-26b-5p. As depicted in Fig. 5C, SNHG6 knockdown significantly reduced ITGB1 protein levels in Eca9706 cells. To assess the interplay between miR-26b-5p, SNHG6, and ITGB1, we examined ITGB1 expression in cells co-transfected with sh-SNHG6 and an miR-26b-5p inhibitor. Consistent with our hypothesis, ITGB1 expression was substantially restored in the co-transfected cells, as shown in Fig. 5C.

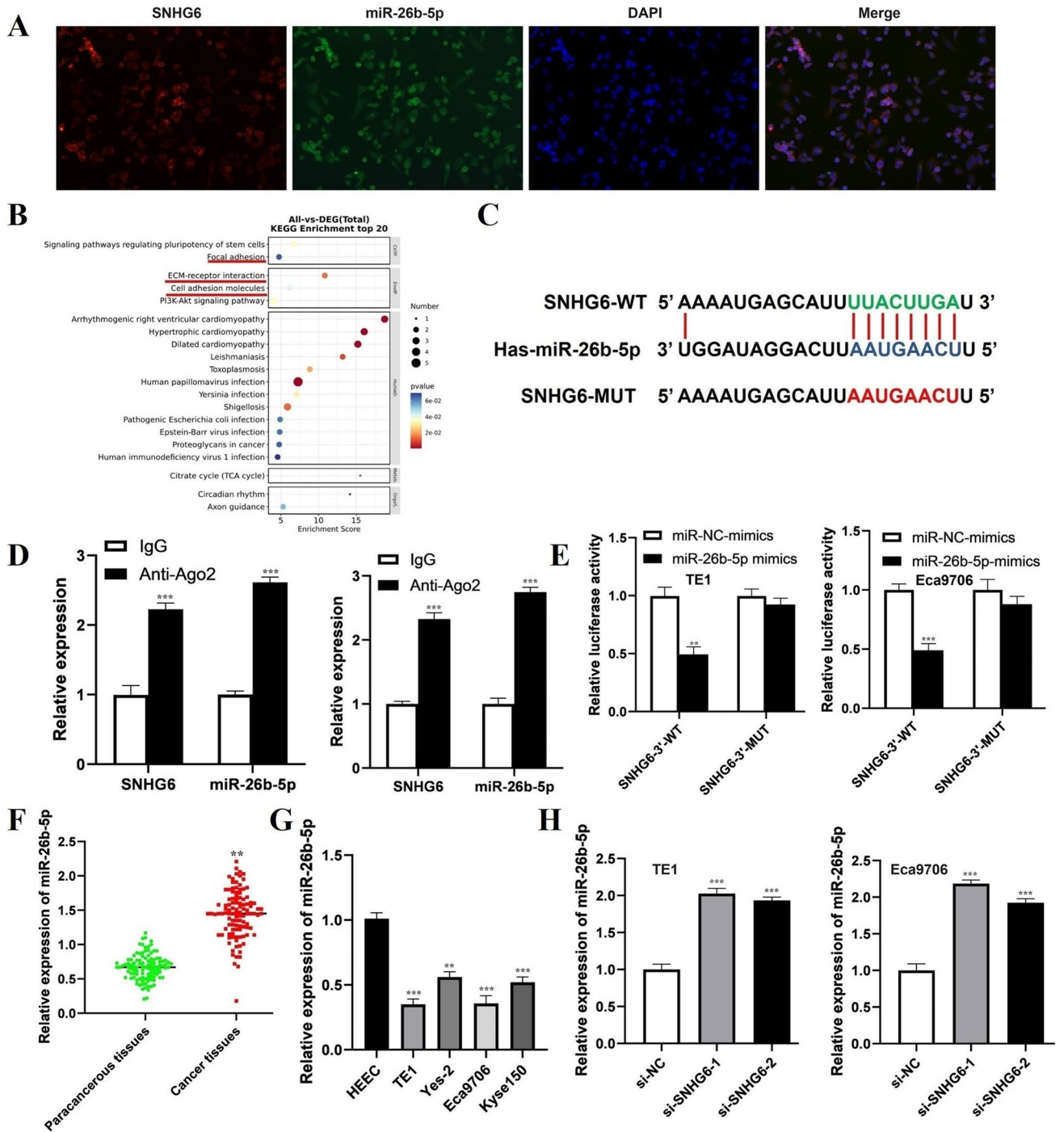


Figure 3. SNHG6 interacts with miR-26b-5p in ESCC cells. **A** SNHG6 and miR-26b-5p localization was detected by FISH assay. **B** KEGG enrichment analysis of the ceRNA network of SNHG6. **C** The binding site of SNHG6 and miR-26b-5p. **D** RIP experiments were performed in TE1 and Eca9706 cells and the coprecipitated RNA was used to quantify SNHG6 and miR-26b-5p expression using qRT-PCR. **E** Luciferase reporter assay showed that miR-26b-5p binds to SNHG6. The luciferase reporter plasmid containing wildtype (Wt) or mutant (Mut) SNHG6 was cotransfected into TE1 and Eca9706 cells with miR-26b-5p mimics or miR-NC mimics. **F** Relative miR-26b-5p expression validated in an independent cohort of 108 pairs of esophageal squamous carcinoma tissues and matched adjacent normal tissues. **G** qRT-PCR analysis of SNHG6 expression in ESCC cells. **H** miR-26b-5p expression by qPCR in TE1 and Eca9706 cells transfected with control siRNA or si-SNHG6. U6 was used as an internal control gene for the quantification of miRNA expression. * $P < 0.05$.

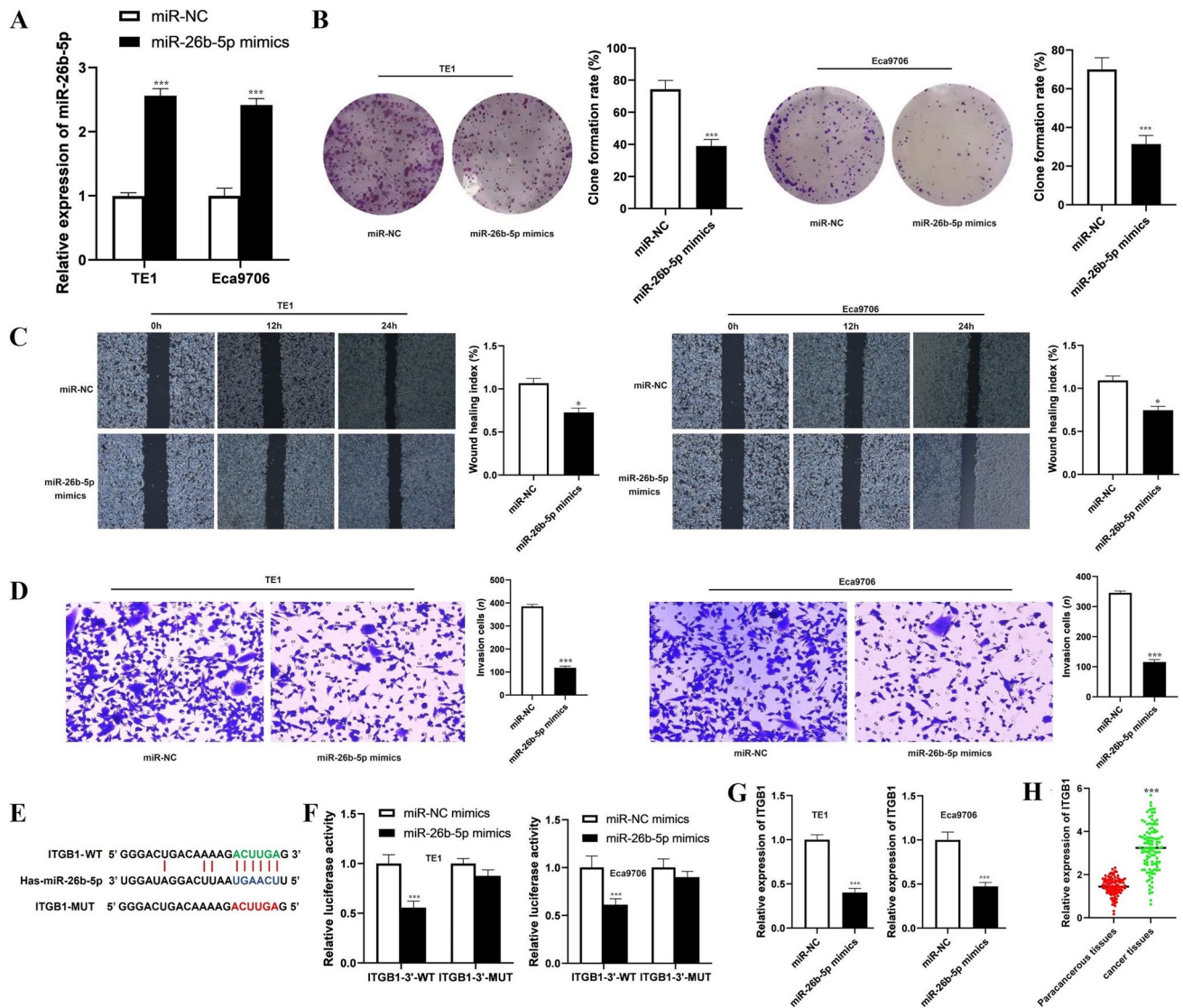


Figure 4. ITGB1 is a target of miR-26b-5p in ESCC. **A** miR-26b-5p expression in ESCC cells transfected with control miRNA or miR-26b-5p mimics was quantified by qRT-PCR. **B** The inhibitory effect of miR-26b-5p mimic on cell proliferation was evaluated using a colony formation assay. **C–D** Migration and invasion ability of ESCC cells transfected with control miRNA or miR-26b-5p mimics. **E–F** Luciferase activity assay in TE1 and Eca9706 cells transfected with plasmid containing ITGB1 3'UTR (wildtype, Wt or mutant, Mut) and miR-26b-5p or control miRNA. **G** qRT-PCR analysis of ITGB1 expression in the TE1 and Eca9706 cells transfected with control miRNA or miR-26b-5p mimics. **H** Relative ITGB1 expression validated in an independent cohort of 108 pairs of esophageal squamous carcinoma tissues and matched adjacent normal tissues. * $P < 0.05$.

Additionally, we explored the function of the SNHG6/miR-26b-5p/ITGB1 axis in vivo. Eca9706 cells, either with reduced SNHG6 or as a negative control, were subcutaneously injected into the back flank of nude mice. The results indicated that the tumor size and weight of the xenograft tumors were significantly lower in the sh-SNHG6 group compared to the negative control group (Fig. 5D–E). A notably lower expression of SNHG6 and higher expression of miR-26b-5p were observed in the SNHG6 knockdown group relative to the negative control group (Fig. 5F–G). We also examined the expression of EMT-related markers. The IHC analysis demonstrated that the knockdown of SNHG6 led to a decrease in the expression levels of Snail and Twist in tumor tissues, concurrently enhancing the expression of E-cadherin (Fig. 5H). These findings suggest the presence of the SNHG6/miR-26b-5p/ITGB1 axis in ESCC. In summary, the SNHG6/miR-26b-5p/ITGB1 axis plays a crucial role in the EMT, metastasis, and progression of ESCC.

Discussion

Esophageal cancer ranks among the most prevalent malignant tumors of the digestive tract in China, accounting for approximately 50% of the global incidence of this disease¹⁸. Despite advances in comprehensive cancer treatment modalities, the 5-year overall survival rate for patients with ESCC remains unsatisfactory. The

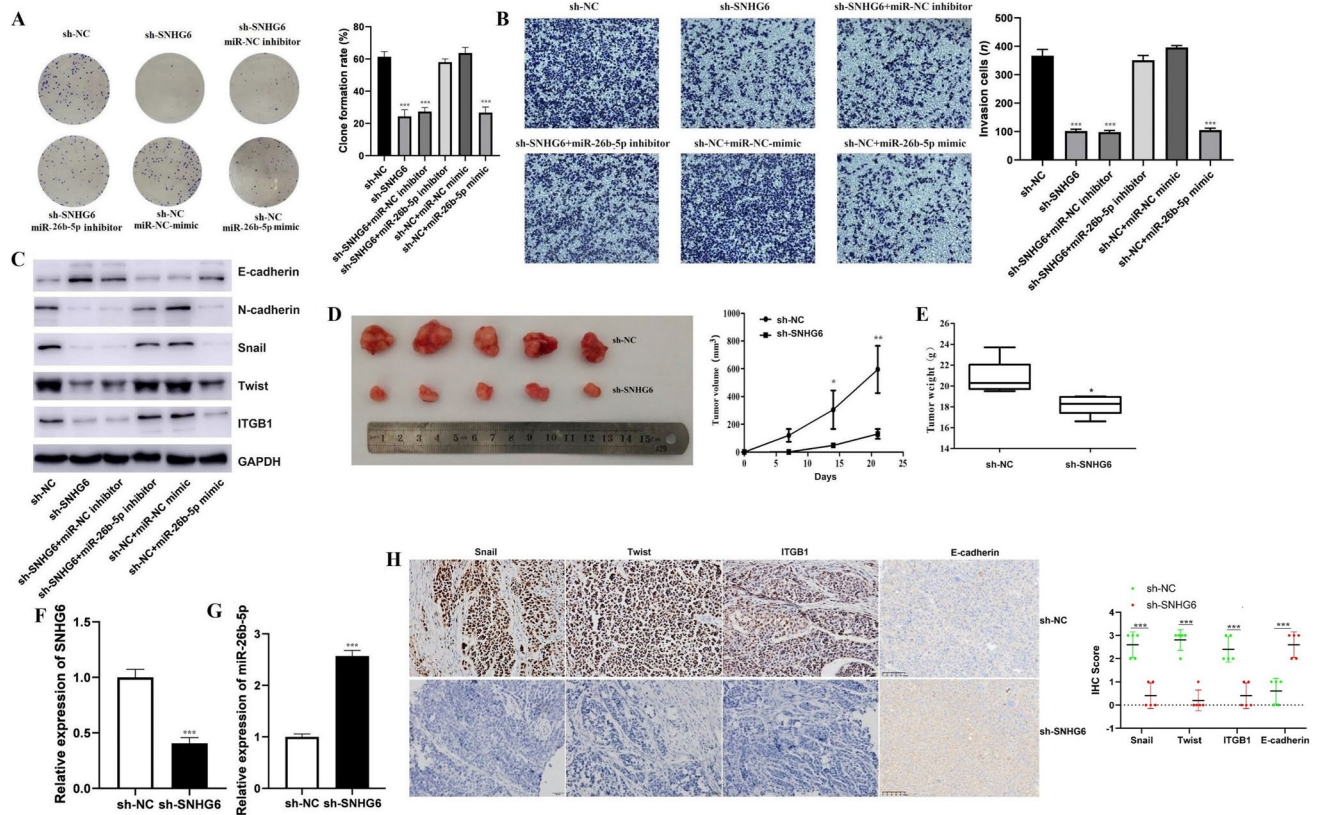


Figure 5. SNHG6 facilitates ESCC cell EMT, metastasis and progression by sponging miR-26b-5p to regulate ITGB1 functions. **A** The effects of SNHG6 knockdown on proliferation ability of Eca9706 cells, assayed with clone formation experiment. **B** The effects of SNHG6 knockdown on migration and invasion ability of Eca9706 cells, assayed with Transwell experiment. **C** The effects of SNHG6 knockdown on E-cadherin, N-cadherin, Snail and Twist expression, assayed with western blotting experiment. miR-26b-5p mimic or inhibitor was used for realizing the indirect effect of SNHG6 on ITGB1. Corresponding miR-NC mimic or inhibitor was used as control. **D-E** Tumor volume and weight of mouse xenografts subcutaneously injected with Eca9706 cells with stable SNHG6 knockdown. The tumor growth curve was measured every 3 days. Nude mice were euthanized 3 weeks following treatment. **F-H** The effect of SNHG6 knockdown on miR-26b-5p, Snail, Twist, E-cadherin and ITGB1 expression via qRT-PCR and IHC *in vivo*. * $P < 0.05$.

activation of EMT is a significant marker of ESCC, associated with poor patient outcomes¹⁹. Emerging research has underscored the pivotal role of lncRNAs in malignancies^{20–24}. Various studies have demonstrated that lncRNA are critically involved in aspects such as transcriptional control, cell differentiation, cell cycle regulation, epigenetics, and developmental processes^{25,26}. Recent evidence suggests that regulatory feedback loops between miRNAs and lncRNAs play substantial roles in the prognosis of malignant tumors^{27,28}. For instance, SNHG8 negatively influences miR-542-3p, impacting NSCLC progression through the regulation of downstream targets like CCND1 and CDK6²⁹. Although the human genome encodes numerous lncRNAs, only a limited number have been experimentally characterized and functionally annotated in ESCC.

In this study, we validated the expression status and function of SNHG6 in ESCC tissues. Previous research by Liang et al. suggested that SNHG6 act as a ceRNA to regulate E2F7 expression by sponging miR-26a-5p in lung cancer³⁰. Moreover, work by Cao et al. proposed that SNHG6 might observe a similar ceRNA role in promoting the progression of hepatocellular carcinoma³¹. Additionally, research by Zhang et al. indicated that SNHG6 could enhance malignancy in ESCC cells¹⁶. To further investigate SNHG6's role in ESCC, we analyzed its expression in ESCC tissues using data from the TCGA database, which confirmed significant overexpression of SNHG6. Subsequent analyses confirmed that SNHG6 was up-regulated in ESCC tissues compared to adjacent normal tissues (Fig. 1A–F, H). Notably, a higher expression of SNHG6 correlates with shorter survival in patients with ESCC (Fig. 1G, I–J), suggesting that SNHG6 is a potential independent prognostic factor for ESCC. Both *in vitro* and *in vivo* experiments indicated that SNHG6 exert a substantial oncogenic effect by promoting ESCC cell growth, migration, invasion, and EMT. There is growing evidence of a broad interaction network involving ceRNAs, where the subcellular localization of lncRNAs affects their function. In our study, SNHG6 was predominantly localized to the cytoplasm and associated with Ago2 in ESCC cells, supporting its role as an endogenous miRNA sponge (Fig. 3C–E). Bioinformatics analysis alongside luciferase reporter assays identified miR-26b-5p, recognized as a tumor suppressor in several cancers including breast, CRC and gastric cancer^{32–34}. Following SNHG6 knockdown, miR-26b-5p expression increased in ESCC cells, consistent with our hypotheses

(Fig. 3H). In conclusion, these findings solidify SNHG6's role as a ceRNA that interacts with miR-26b-5p in ESCC cells.

The role of miR-26b-5p in ESCC has been relatively underexplored. In this study, we propose that overexpression of miR-26b-5p in ESCC cell line inhibits cell proliferation and metastasis (Fig. 4A–D). Our findings reveal the interaction between SNHG6 and miR-26b-5p in ESCC tumorigenesis, with SNHG6 partly exerting its oncogenic effects by sponging miR-26b-5p in these cells (Fig. 5A–C). Initially, we employed bioinformatics analysis to predict miR-26b-5p targets, which we subsequently validated through a luciferase assay. We identified ITGB1 as the primary target, and its overexpression can induce EMT in cancer cells, contributing to the malignant progression in various epithelial tumors^{35,36}. Furthermore, ITGB1 mRNA status were modulated by miR-26b-5p in cell lines (Fig. 4G). The RT-qPCR results from our study indicated that high ITGB1 expression in ESCC tissues (Fig. 4H) positively associated with SNHG6 (Supplemental Fig. 1A) and inversely correlated with miR-26b-5p (Supplemental Fig. 1B). Given its prevalence in ESCC tissues and its role in regulating cell migration and EMT, we hypothesized that SNHG6 could regulate ITGB1 expression by competitively sponging miR-26b-5p, thus promoting ESCC cell invasion and EMT. To evaluate SNHG6's role in the lncRNA-miRNA-mRNA model, we conducted correlation experiments that demonstrated a decrease in ITGB1 mRNA and protein levels following SNHG6 knockdown, a decrease that miR-26b-5p mimics could rescue (Fig. 5C). Functional assays confirmed these results. These findings suggest that SNHG6 regulates ITGB1 expression by sponging miR-26b-5p and impacts the biological behavior of ESCC cells by modulating EMT-related markers. Specifically, SNHG6 knockdown increased epithelial marker protein E-cadherin expression, while reducing interstitial protein expressions of N-cadherin, Snail, and Twist, thereby significantly inhibiting EMT through the miR-26b-5p/ITGB1 axis (Fig. 5C).

To the best of our knowledge, this study is the first to validate the impact of SNHG6 on EMT and its associated mechanisms in ESCC. SNHG6 was found to be highly expressed in ESCC, and its overexpression correlated with a poor prognosis in patients. The knockdown of SNHG6 significantly inhibited the malignant biological behaviors, including EMT, in ESCC cells. Moreover, suppression of SNHG6 negated the inhibitory effect could be reversed by a miR-26b-5p mimic. Our findings suggest that SNHG6 may act as a ceRNA, indirectly regulating ITGB1 by interacting with miR-26b-5p. We have thoroughly explored the mechanism of the SNHG6/miR-26b-5p/ITGB1 axis in ESCC, providing new theoretical insights into ESCC metastasis and identifying a novel target for improving outcomes in metastatic ESCC.

Materials and methods

Patients and specimens This study was approved by the Medical Ethics Committee of the Fourth Affiliated Hospital of Hebei Medical University (2022KS043), conformed to the Declaration of Helsinki. Informed consent was available for each patient. Tissue specimens from ESCC and adjacent non-cancerous tissues were collected from 108 patients who underwent surgical procedures at the Fourth Hospital of Hebei Medical University (Shijiazhuang, China) between February 2018 and September 2019. These patients had not received any anti-tumor treatments, such as radiation therapy, chemotherapy or immunotherapy prior to surgery. ESCC and adjacent non-cancerous tissue samples were immediately processed post-surgery, frozen within 30 min and stored at -80 °C for RNA extraction. The study was approved by the Ethics Committee of Hebei Medical University and informed consent was obtained from all patients before surgery.

Cell culture The ESCC cell lines (TE1, Yes-2, Eca9706, KYSE150) and normal esophageal epithelial cells (HEEC) were maintained at the Research Center of the Fourth Hospital of Hebei Medical University. All cell lines were cultured in RPMI1640 medium supplemented with 10% FBS, penicillin (100 U/ml), and streptomycin (100 µg/ml), and incubated at 37°C in a humidified atmosphere with 5% CO₂.

Cell transfection Hsa-miR-26b-5p mimic, negative control mimic, miR-26b-5p inhibitor and negative control inhibitor were procured from Applied Biological Materials (GenePharma, Shanghai, China). The sequence of has-miR-26b-5p mimics: UUCAAGUAAUUCAGGAUAGGUCUAUCCUGAAUUACUUGAAUU. The sequence of has-miR-26b-5p inhibitor: ACCUAUCCUGAAUUACUUGAA. The siRNA sequences targeting SNHG6 included si-SNHG6-1, 5'-GAAGGUGUAUGAAAGUCAUTT-3'; si-SNHG6-2, 5'-GCGGCAUGUAUUGAG CAUATT-3' and si-SNHG6-3, 5'-GUUACCUCAAGUGUGGCAUTT-3'. The negative control sequence was si-NC, 5'-UUCUCCGAACGUGUCACGUTT-3'. The shRNA sequences targeting SNHG6 (vector: pHBLV-U6-MCS-CMV-ZsGreen-PGK-PURO) included sh-SNHG6-1, 5'-GCGGCAUGUAUUGAGCAUATT-3'; sh-SNHG6-2, 5'-GAAGGUGUAUGAAAGUCAUTT-3' and sh-SNHG6-3, 5'-GUUACCUCAAGUGUGGCAUTT-3'. The negative control sequence was sh-NC, 5'-UUCUCCGAACGUGUCACGUTT-3'. Transfections were conducted using the Lipofectamine 3000 kit (Invitrogen), adhering to the manufacturer's instructions.

RNA isolation and real-time quantitative reverse transcription Total RNA was isolated from tissues and cells using Trizol reagent (Invitrogen, CA, USA) following the manufacturer's instructions and was reverse-transcribed into cDNA using TaqMan MultiScribe Reverse Transcriptase (Applied Biosystems, Foster City, CA, USA). Real-time quantitative polymerase chain reaction (qRT-PCR) was conducted using the SYBR kit as per the manufacturer's guidelines. The primer sequences for SNHG6 and GAPDH are provided in Supplement Table 1. Expression levels of miR-26b-5p, SNHG6, and ITGB1 mRNA were determined using the 2^{-ΔΔCt} method and normalized to U6 and GAPDH mRNA, respectively. All assays were performed in triplicate.

Cell Proliferation assay Cell clone formation assays assess the proliferative capacity of ESCC cell lines. The transfected cells were seeded into 6-well plates at a density of 1 × 10³ cells. After 2 to 3 weeks of routine culturing,

fixation was conducted. Colonies consisting of more than 50 cells were counted under a microscope, and the colony formation rate was subsequently calculated. This experiment was conducted in triplicate.

Wound healing assay Wound healing was utilized to assess the migratory capacity of ESCC cell lines. The forementioned cells were cultured in a 6-well plate, with the cell density adjusted to 5×10^5 . Upon reaching 80% confluence, a sterile micropipette tip was used to create a scratch wound on each plate. The medium was subsequently replaced with a serum-free alternative, and phase-contrast images of the same scratch location were captured using an inverted microscope at 0, 12, and 24 h. This experiment was replicated three times.

Transwell assay The invasive capacity of ESCC cell lines was assessed using the Transwell assay. Initially, 50 μ l of Matrigel was layered onto the upper Transwell chamber. Subsequently, 5×10^4 cells were seeded in 200 μ l of RPMI1640 medium devoid of fetal bovine serum in the upper chamber, while 500 μ l of RPMI 1640 medium with 10% fetal calf serum was added to the lower chamber. Following a 24-hour incubation period, cells on the lower surface of the chamber were fixed, stained, and quantified using an inverted microscope. This procedure was replicated three times.

RNA immunoprecipitation (RIP) assay RIP was conducted using a Magna RIP RNA-Binding Protein Immunoprecipitation Kit (Millipore, Billerica, MA, USA) according to the manufacturer's instructions, with minor modifications. Specifically, an antibody against Ago2 (Abcam, Cambridge, MA, USA) was employed. The co-precipitated RNAs were captured with magnetic beads and analyzed via qRT-PCR. Concurrently, total RNAs (input controls) and the antibody isotype control rabbit IgG were utilized to confirm that the signals detected originated specifically from RNAs binding to protein Ago2.

Dual luciferase reporter assay PmirGLO-SNHG6-wt or pmirGLO-SNHG6-mut was co-transfected with miR-26b-5p mimics or miR-NC into HEK293 cells via lipofectamine-mediated gene transfer. The relative luciferase activity was normalized to renilla luciferase activity 48 h post-transfection.

Tumorigenesis in nude mice The care provided adhered to the National Research Council Guide for the Care and Use of Laboratory Animals and received approval from the Institutional Animal Care and Use Committee (IACUC) of Hebei Medical University, Shijiazhuang, China. The study is reported in accordance with ARRIVE guidelines. BALB/c nude mice aged 4–6 weeks were utilized for in vivo tumor growth assays. A total 5.0×10^6 tumor cells, transfected with sh-SNHG6 or sh-NC, were collected using trypsin solution, suspended in 100 μ l of PBS, and subcutaneously injected into the flank of each mouse. Tumor size was measured once a week using vernier calipers as $(\text{length} \times \text{width}^2)/2$. In this study, no animals were subjected to anesthesia. Mice were euthanized by cervical dislocation at endpoint, which was either signs of tumor growth (e.g., hunched back, weight loss, head tilt, etc.) or five weeks after transplantation. Subsequently, the primary tumors were extracted, weighed, and processed for further histological analysis.

Immunohistochemistry (IHC) assay IHC was conducted and analyzed following previously established protocols⁷. The primary antibodies utilized were as follows: anti-Snail, anti-Twist, anti-ITGB1, and anti-E-cadherin. Staining evaluation was performed using the IHC Profiler in ImageJ. Staining scores of 0 and 1+ were classified as negative expression, while scores of 2+ and 3+ were classified as positive expression.

Western blot assay Western blot analysis was utilized to assess protein expression levels in ESCC cell lines. Cells were cultured for 48 h, following which proteins were extracted and quantified using BCA method. Subsequently, 30 μ g of total protein from each sample was subjected to 10% SDS-PAGE and transferred onto a PVDF membrane. The membrane was blocked with 5% skim milk at room temperature and incubated with primary antibodies against ITGB1 (1:1000), E-cadherin (1:1000), N-cadherin (1:1000), Snail (1:500), and Twist (1:500), followed by incubation with goat anti-rabbit and goat anti-mouse secondary antibodies. The membranes were analyzed using Quantity One 4.6 software with GAPDH serving as the internal control. The relative expression of the protein was quantified based on the gray value ratio of each protein band.

Statistical analysis Statistical analyses were conducted using SPSS Statistics software, version 25.0 (SPSS, Chicago, IL, USA). All measurement data were presented as mean \pm SD. Correlations between SNHG6 expression and clinical characteristics were evaluated by using the Kendall rank test. Student t-test was used for analyzing the measurement data. Survival analyses were performed using the log-rank test in conjunction with Kaplan-Meier analysis and the Cox proportional hazards model. Pearson correlation was used to analyze the associations between SNHG6, miR-26b-5p and ITGB1 in ESCC tissue specimens. A P value < 0.05 was considered statistically significant.

Data availability

The data used to support the findings of this study are available from the corresponding author request.

Received: 23 July 2024; Accepted: 14 October 2024

Published online: 23 October 2024

References

1. Siegel, R. L. et al. Cancer statistics, 2024. *CA J. Clin.* **74** (1), 12–49 (2024).

2. Puhr, H. C. et al. How we treat esophageal squamous cell carcinoma. *EMSO Open*. **8** (1), 100789 (2023).
3. Herman, A. B. et al. Integrated lncRNA function upon genomic and epigenomic regulation. *Mol. Cell*. **82** (12), 2252–2266 (2022).
4. Bridges, M. C. et al. LNCcation: lncRNA localization and function. *J. Cell. Biol.* **220** (2), e202009045 (2021).
5. Nojima, T. et al. Mechanisms of lncRNA biogenesis as revealed by nascent transcriptomics. *Nat. Rev. Mol. Cell. Biol.* **23** (6), 389–406 (2022).
6. Yip, C. W. et al. Functional annotation of lncRNA in high-throughput screening. *Essays Biochem.* **65** (4), 761–773 (2021).
7. Li, Y. et al. A wnt-induced lncRNA-DGCR5 splicing switch drives tumor-promoting inflammation in esophageal squamous cell carcinoma. *Nat. Commun.* **42** (6), 112542 (2023).
8. Cui, Y. et al. RNA m6A demethylase FTO-mediated epigenetic up-regulation of LINC00022 promotes tumorigenesis in esophageal squamous cell carcinoma. *J. Exp. Clin. Cancer Res.* **40** (1), 294 (2021).
9. Liu, J. et al. Long noncoding RNA regulating immune escape regulates mixed lineage leukemia protein-1-H3K4me3-mediated immune escape in esophageal squamous cell carcinoma. *Clin. Transl. Med.* **13** (9), e1410 (2023).
10. Xue, S. T. et al. Long non-coding RNA LINC00680 functions as a ceRNA to promote esophageal squamous cell carcinoma progression through the miR-423-5p/PAK6 axis. *Mol. Cancer*. **21** (1), 69 (2022).
11. Liu, Y. et al. Lipid metabolism-related lncRNA SLC25A21-AS1 promotes the progression of esophageal squamous cell carcinoma by regulating the NPM1/c-Myc axis and SLC25A21 expression. *Clin. Transl. Med.* **12** (6), e944 (2022).
12. Liu, J. et al. Long noncoding RNA AGPG regulates PFKFB3-mediated tumor glycolytic reprogramming. *Nat. Commun.* **11** (1), 1507 (2020).
13. Yu, M. X. et al. N4-acetylcytidine modification of lncRNA CTC-490G23.2 promotes cancer metastasis through interacting with PTBP1 to increase CD44 alternative splicing. *Oncogene*. **42** (14), 1101–1116 (2023).
14. Xue, W. et al. Long non-coding RNAs MACC1-AS1 and FOXD2-AS1 mediate NSD2-induced cisplatin resistance in esophageal squamous cell carcinoma. *Mol. Ther. Nucleic Acids*. **23**, 592–602 (2020).
15. Guo, K. et al. LncRNA-MIAT promotes thyroid cancer progression and function as ceRNA to target EZH2 by sponging miR-150-5p. *Cell. Death Dis.* **12** (12), 1097 (2021).
16. Zhang, Y. et al. Upregulation of long non-coding RNA SNHG6 promote esophageal squamous cell carcinoma cell malignancy and its diagnostic value. *Am. J. Transl. Res.* **11** (2), 1084–1091 (2019).
17. Wang, Y. Q. et al. LncRNA SNHG6 promotes breast cancer progression and epithelial-mesenchymal transition via miR-543/LAMC1 axis. *Breast Cancer Res. Treat.* **188** (1), 1–14 (2021).
18. Chen, Y. et al. Epithelial cells activate fibroblasts to promote esophageal cancer development. *Cancer Cell*. **41** (5), 903–918 (2023).
19. Guo, X. et al. EIF3H promotes aggressiveness of esophageal squamous cell carcinoma by modulating snail stability. *J. Exp. Clin. Res.* **39** (1), 175 (2020).
20. Mercer, T. R. et al. Long non-coding RNAs: insights into functions. *Nat. Rev. Genet.* **10** (3), 155–159 (2009).
21. Tsai, M. C. et al. Long noncoding RNA as modular scaffold of histone modification complexes. *Science*. **329** (5992), 689–693 (2010).
22. Bhan, A. et al. Long noncoding RNA and cancer: a new paradigm. *Cancer Res.* **77** (15), 3965–3981 (2017).
23. Zhang, A. et al. Role of the lncRNA-p53 regulatory network in cancer. *J. Mol. Cell. Biol.* **6** (3), 181–191 (2014).
24. Chen, K. et al. High lncRNA MEG3 expression is associated with high mortality rates in patients with sepsis and increased lipopolysaccharide-induced renal epithelial cell and cardiomyocyte apoptosis. *Exp. Ther. Med.* **18** (5), 3943–3947 (2019).
25. Yu, B. X. et al. LncRNA SAMD12-AS1 down-regulates P53 to promote malignant progression of glioma. *Eur. Rev. Med. Pharmacol. Sci.* **23** (19), 8456–8467 (2019).
26. McCabe, E. M. et al. LncRNA involvement cancer stem cell function and epithelial-mesenchymal transitions. *Semin Cancer Biol.* **75**, 38–48 (2021).
27. Militello, G. et al. Screening and validation of lncRNAs and circRNAs as miRNA sponges. *Brief. Bioinform.* **18** (5), 780–788 (2017).
28. Yan, H. et al. Non-coding RNA in cancer. *Essays Biochem.* **65** (4), 625–639 (2021).
29. Chen, C. et al. SNHG8 is identified as a key regulator in non-small-cell lung cancer progression sponging to mir-542-3p by targeting CCND1/CDK6. *Onco Targets Ther.* **11**, 6081–6090 (2018).
30. Liang, R. et al. SNHG6 functions as a competing endogenous RNA to regulate E2F7 expression by sponging miR-26a-5p in lung adenocarcinoma. *Biomed. Pharmacother.* **107**, 1434–1446 (2018).
31. Cao, C. et al. The long non-coding RNA, SNHG6-003, functions as a competing endogenous RNA to promote the progression of hepatocellular carcinoma. *Oncogene*. **36** (8), 1112–1122 (2017).
32. Ma, S. et al. MiR-26b-5p inhibits cell proliferation and EMT by targeting MYCBP in triple-negative breast cancer. *Cell. Mol. Biol. Lett.* **26**(1), 52 (2021).
33. Guo, S. et al. LncRNA HCG11 promotes colorectal cancer cell malignant behaviors via sponging miR-26b-5p. *J. Immunol. Res.* **2023**, 9011232 (2023).
34. Xu, T. et al. Loss of miR-26b-5p promotes gastric cancer progression via miR-26b-5p-PDE4B/CDK8-STAT3 feedback loop. *J. Transl. Med.* **21** (1), 77 (2023).
35. Wang, N. et al. Maspin suppresses cell invasion and migration in gastric cancer through inhibiting EMT and angiogenesis via ITGB1/FAK pathway. *Hum. Cell.* **33** (3), 663–675 (2020).
36. Li, Y. et al. ITGB1 enhances the radioresistance of human non-small cell lung cancer cells by modulating the DNA damage responses and YAP1-induced epithelial-mesenchymal transition. *Int. J. Biol. Sci.* **17** (2), 635–650 (2021).

Acknowledgements

No.

Author contributions

L.J. Wang, Y.L. Jia and L.H. Liu designed research; J.L. Wang, J.X. Si, Z.Y. Zhao and C.L. Gao performed research and analyzed data; J.L. Wang, T.X. Liu and L.H. Liu wrote the paper; Y.L. Jia and L.H. Liu obtained funding. All authors reviewed the manuscript.

Funding

This research is supported by the National Natural Science Foundation of China (82203079), Clinical Research and Innovation Team Support Program of Hebei Medical University (2022LCTD-A11), and Research and Innovation Team Support Program of Hebei Medical University (2023C11).

Declarations

Ethical approval

The human study was approved by the Medical Ethics Committee of Fourth Affiliated Hospital of Hebei Medical University (2022KS043), conformed to the Declaration of Helsinki. The animal study was approved by the Laboratory Animal Welfare and Ethics Committee of the Fourth Affiliated Hospital of Hebei Medical University and followed the guide for the Care and Use of Laboratory Animals published by the US National Institutes of Health.

Competing interests

The authors declare no competing interests.

Additional information

Supplementary Information The online version contains supplementary material available at <https://doi.org/10.1038/s41598-024-76521-8>.

Correspondence and requests for materials should be addressed to L.L.

Reprints and permissions information is available at www.nature.com/reprints.

Publisher's note Springer Nature remains neutral with regard to jurisdictional claims in published maps and institutional affiliations.

Open Access This article is licensed under a Creative Commons Attribution-NonCommercial-NoDerivatives 4.0 International License, which permits any non-commercial use, sharing, distribution and reproduction in any medium or format, as long as you give appropriate credit to the original author(s) and the source, provide a link to the Creative Commons licence, and indicate if you modified the licensed material. You do not have permission under this licence to share adapted material derived from this article or parts of it. The images or other third party material in this article are included in the article's Creative Commons licence, unless indicated otherwise in a credit line to the material. If material is not included in the article's Creative Commons licence and your intended use is not permitted by statutory regulation or exceeds the permitted use, you will need to obtain permission directly from the copyright holder. To view a copy of this licence, visit <http://creativecommons.org/licenses/by-nc-nd/4.0/>.

© The Author(s) 2024